

MORPHOLOGY, COMPOSITION, AND SUPERCOOLING, OF THE PRIMARY OLIVINE MICROCRESCUMULATE FROM THE LIZARD PERIDOTITE, CORNWALL.

A.T.V.ROTHSTEIN

Morphology, composition, and supercooling of the primary olivine microcrescumulate from the Lizard peridotite, Cornwall. *Geoscience in south-west England*, **10**, 086-091



The primary assemblage Lizard peridotites show a textural range, from those with many relic primary textures, including both microcrescumulates and cumulates, but with some deformation and recrystallization, to others which are peridotite tectonites with porphyroclastic textures. Both groups have mineral assemblages characteristic of the spinel-lherzolite facies of the upper mantle, and have been shown to fall on a declining P-T trajectory. The pyroxenes present in the first group give original temperatures of equilibration approaching $1200\text{ }^{\circ}\text{C} \pm 70^{\circ}\text{C}$ and $15\text{Kb} \pm 41\text{Kb}$. Mineral analyses of the co-existing pyroxene and spinel from these rocks have been published.

The microcrescumulates contain olivine crystals whose morphology ranges from polyhedral to hopper, and from euhedral to rounded. The cumulates contain relics of rounded olivines. The spinels, which occur in both microcrescumulates and cumulates, show an associated range of morphologies from polyhedral to hopper and dendritic. The pyroxenes, which occur interstitially within the olivine microcrescumulate framework, show relics of polyhedral morphologies. These diverse features indicate a moderate degree of supercooling in the initial crystallization of the primary precipitate.

Fresh olivine from harzburgites has been analysed, both from well preserved microcrescumulate structures in a relatively undeformed rock and from relic primary textures set in a more deformed matrix. The olivine appears to be that of a non-komatiitic suite of ultramafic plutonic igneous rocks.

A.T.V.Rothstein, 12 Court Lane, Cosham, Portsmouth, Hants. P06 2LN

INTRODUCTION

In a series of publications numerous mineralogical and textural features of the primary assemblage peridotites of the Lizard, Cornwall have been described (Flett, 1946; Green, 1964a & b; Rothstein 1977, 1981, 1988, 1994, 1998; Cook *et al*, 1998; Davies, 1984). Flett (1946) wrote 'It is doubtful whether there is any serpentine of normal igneous structure in the Lizard. The usual poikilitic or poikilo-porphyratic structure of peridotites has never been observed in typical development, though traces of it are sometimes provided by large enstatite crystals that carry in their interior rounded grains of olivine. Moreover the large enstatites are never idiomorphic but always phacoidal, often broken and embedded in a matrix of olivine, pyroxene and amphibole developed by movement and friction.'

Later papers have shown that the primary assemblage peridotites of the Lizard, Cornwall contain overall olivine + spinel + Ca-poor pyroxene + Ca-rich pyroxene, and contain a range of textures. At one end of the range of textures are those rocks with many diverse relics of somewhat unusual complex primary textures. Many examples of such rocks are found in some of the outcrops with a mineralogical banding, particularly in harzburgites. These primary textures are often at steep angles to a primary layering (So). The author has argued that these textures indicate precipitation from a melt (Rothstein, 1981). This paper describes in detail the olivine morphology, and in part the morphology of the spinels, of these primary textures. From this morphological evidence it is concluded that, in part, precipitation occurred under conditions of supercooling. These rocks may also show some deformation and recrystallization. At the other end of the textural range are those rocks which, while consisting overall of the primary assemblage minerals, are heavily deformed with secondary planar and linear fabrics and porphyroclastic textures and are peridotite tectonites. Relics of the primary textures may be discerned in some of these deformed rocks.

Using the equations of Wells (1977), Mercier (1980), and Witt-Eikschon and Seck (1991) and the data presented in Table 2, the pyroxenes present in those rocks with primary textures indicate

temperatures and pressures of an original equilibration approaching $1200\text{ }^{\circ}\text{C} \pm 70\text{ }^{\circ}\text{C}$, and $15\text{Kb} \pm 4\text{kb}$. These values are characteristic of the spinel-lherzolite facies of the upper mantle under oceanic crust. Furthermore, these values have been shown to be the initial points of a declining P-T trajectory for the primary assemblage peridotite as a whole as deformation and recrystallization developed. Analyses of the co-existing pyroxene and spinel from primary assemblage peridotites with relic primary textures have been published (Rothstein, 1981, 1988, 1998).

THE PRIMARY TEXTURES

The primary textures themselves can be divided into two varieties; microcrescumulate and those with a cumulate appearance. These various textures are particularly well preserved in outcrops of banded rocks between Downas Cove and Pedn Boar, at localities H3, H, and Z (Fig. 1). The olivine microcrescumulates (Rothstein, 1981) are on the whole on a millimetre scale but there are one or two exceptions. The cumulate appearance is associated with the disposition of particular trails of spinels at localities H3 and Z (Rothstein, 1994, 1998). The microcrescumulates have principally been found within the harzburgites of the interbanded outcrops of harzburgite and pyroxenite at locality H. These microcrescumulates are found in outcrops occurring over a distance of 6 metres across the strike. These harzburgites often contain a small amount of Ca-rich pyroxene. The cumulates which occur within the dunite of the interbanded dunite and harzburgite (localities H3 and Z) also show associated microcrescumulate features.

The banded outcrops referred to above, at H3, H, and Z, have consistent growth (younging) directions of development of the primary structures and textures. This direction is from west to east. It should also be noted that some of those primary assemblage peridotites between Downas Cove and Pedn Boar which do not show a mineralogical banding have somewhat more deformed and recrystallized textures, but many primary relics are present.

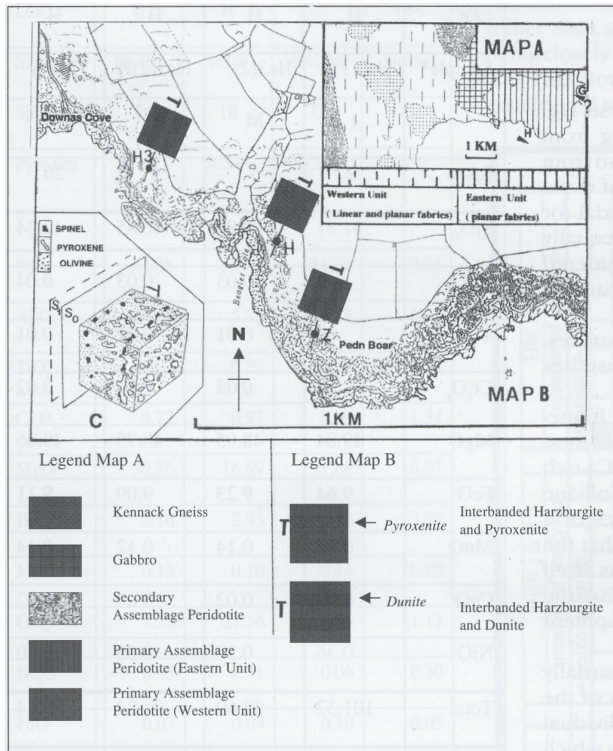


Figure 1. Location map

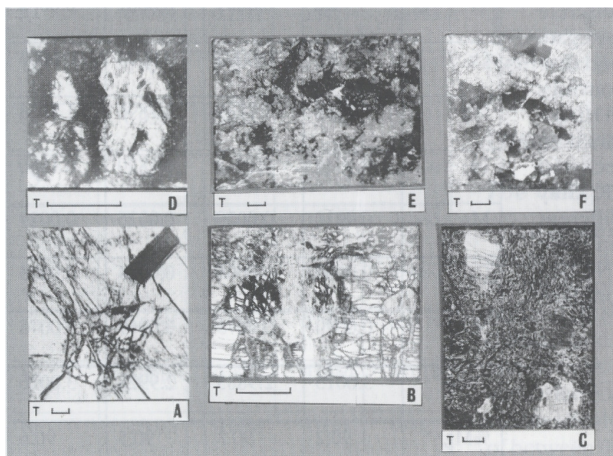


Figure 2. Examples of the Range of Olivine Morphology [Location H] [Scale bars are 1mm, except for A in which scale bar is 0.1 mm]

- Euhedral olivine [harzburgite-Hg]. Note also the euhedral spinet. Both OL and Sp enclosed in OP.
- Subhedral to rounded olivine [harzburgite-Hb]. The olivine crystal is subparallel to S_0 . Enclosed in OP.
- The outlines of rounded subhedral olivines may be seen to be at a steep angle to S_0 [harzburgite-Hc]. The white area is OP.
- Hopper olivine, perpendicular to S_0 [harzburgite-He3]. This hopper is immediately following the pyroxenite [He2].
- Hopper olivine with budding [harzburgite-He1]. Note the development of curvature in the hopper structure.
- Extended hopper olivine and also recurved hopper olivine, the latter arising from increasingly uneven growth as the crystal developed [harzburgite-He3].

NB: In D, E, and F the OP appears black/grey.

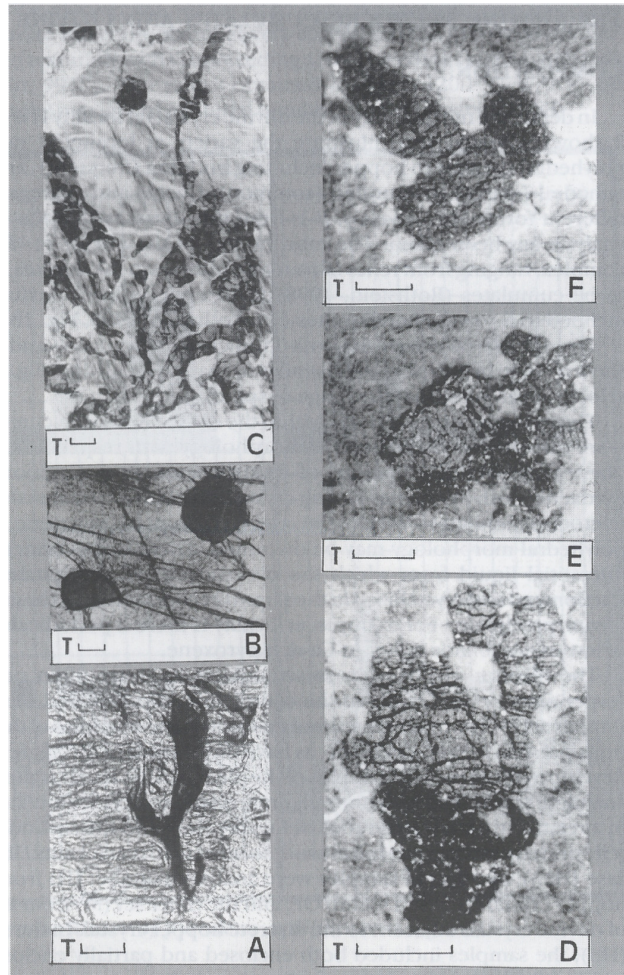


Figure 3. Ranges of Spinel Morphology [locations H and H3.1] [Scale bars are 1mm, except for A and C in which the scale bar is 0.1 mm]

Examples of range of spinel morphology at H:

In the overall sequence [Hc-He2-He3] (harzburgite, pyroxenite, harzburgite), from west to east, the spinel morphology ranges from hopper/dendritic to polyhedral to hopper/dendritic.

- Development of recurved spinel (hopper/dendritic) arising from a budding spinel structure (harzburgite [Hc]).
- Euhedral spinel enclosed in OP (pyroxenite [He2]). The overall assemblage of the pyroxenite is OP + CLP + SP.
- Hopper/dendritic spinel enclosed in OP (harzburgite [He3]). This spinet texture is considered to have arisen as the result of morphological instability developing during growth.

Examples of spinel morphology at H3:

(Within the spinel-bearing dunite H3e, the sequence shown is in the direction of development of the dunite He3, that is from west to east.)

The overall sequence [D - E - F] ranges from hopper (budding) to polyhedral.

- Budding spinel structure (left hand side of dunite)
- Polyhedral spinel (with relics of growth texture) within a tenuous spinel layer
- Polyhedral spinel with sieve texture (for more details of spinel morphology and spinet composition at H3 see Rothstein [1998]).

THE OLIVINE MICRORES CUMULATES AND OLIVINE COMPOSITION

In detail, the morphology of the olivine crystals at locality H is diverse. Fig. 2 shows a selection to illustrate the variety at locality H ranging from polyhedral (scarce) to hopper including budding (frequent), and also from euhedral (scarce) to rounded (common). Chains and aggregates of these different forms also develop. It is from this diversity that the material for analysis has been taken. The morphology of the olivine at H3 is equally complex, ranging from relics of rounded olivines in the dunites, considered to be cumulates (Rothstein, 1998) to extended olivine textures, steeply inclined to S_0 , in the harzburgites (see Rothstein, 1998, Fig. 2B).

The spinels, which occur both in microrescumulates and cumulates, show a range of morphologies similar to that of the olivine. Fig. 3 illustrates selected examples from the range of spinel morphologies.

The pyroxenes which occur within the olivine microrescumulate framework mainly have an interstitial morphology with respect to the olivines. There is an overall sequence of crystallization from Ca-poor to Ca-rich pyroxene; both pyroxenes having crystallized within a framework of olivine microrescumulates. Within the areas of Ca-poor pyroxene, relics of a polyhedral morphology may be discerned. There is also evidence that the interstitial liquid from which the pyroxenes have precipitated has itself fractionated and crystallized in the same direction as that of the growth of the olivine precipitate. For example, at locality H there is periodic development of lenses and bands richer in Ca-rich pyroxene.

The olivines of the microrescumulates at H are often only partially serpentinized, in contrast to the completely serpentinized olivines of the dunites at H3. The microrescumulates have many examples of the individual units preserved as fresh olivine, as have the olivines of the aggregates which develop in these rocks. Examples of the olivine in the harzburgites have been analysed; the first being from well preserved microrescumulate structures in a relatively undeformed rock at locality He3; and the second being from relic primary textures set in a more deformed matrix at locality Hb. In the first case (He3), two sets of samples were analysed; one set (H) from a discrete hopper crystal enclosed within OP, and the other set (M) from an aggregate of olivine crystals adjacent to the discrete hopper crystal. In the second case (Hb), the samples included both enclosed and partially enclosed olivines within OP. The range and type of relic primary olivine morphologies in Hb are closely similar to many of those found in He3. For example, small branching hopper chains of somewhat rounded olivine and also a completely recurved extended olivine hopper crystal are preserved within areas of OP. Only relatively small non-systematic variations were found between the different groups of spot analyses from He3 and Hb. These analyses are set out in Table 1. Fig. 4 shows the range of individual spot values for wt% Mg v. wt% Ni. This plot includes the spot probe values for the analysed olivine (i) from He3 (Rothstein, 1981).

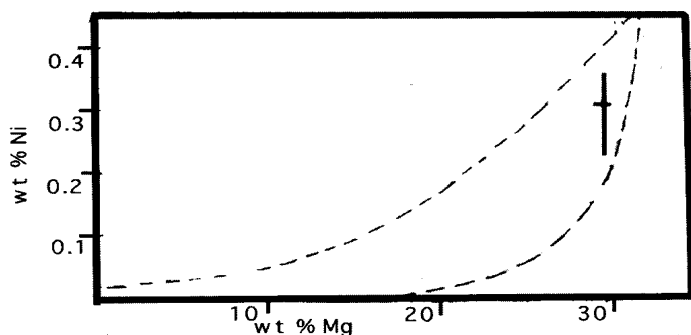


Figure 4. Plot of wt%Mg v. wt% Ni

Analyses of the co-existing pyroxenes with these olivines have been undertaken (see Table 2), giving values for a temperature of an initial equilibration. The range of values for the individual probe spots is also shown in Fig. 5, and the position of the values obtained from the averaged analyses of Table 2 are also indicated. These temperatures overall are not as high as those calculated previously for the pyroxenite Het (Rothstein, 1988), but some of the probe spots currently obtained do have high values. From the

LOC.	H	H	H	H
Sample*	He3(1)(i)	He3(2)	He3(2)H	Hb(1)
)	M		
Spots	3	5	5	26
SiO ₂	41.31	40.8	40.85	40.34
Al ₂ O ₃	nd	0.03	0.03	0.04
TiO ₂	nd	0.01	0.02	0.01
Cr ₂ O ₃	nd	0.03	0.02	0.02
MgO	49.84	48.05	48.75	49.06
FeO	9.64	9.23	9.09	9.11
MnO	0.15	0.14	0.12	0.14
CaO	0.02	0.02	0.01	0.02
NiO	0.36	0.38	0.35	0.4
Total	101.32	98.69	99.24	99.14
Si	0.999	1.0105	1.0057	0.9961
Al	nd	0.001	0.0008	0.001
Ti	nd	0.0002	0.0002	0.0002
Cr	nd	0.0005	0.0003	0.0003
Mg	1.7968	1.7739	1.789	1.8058
Fe	0.1949	0.1912	0.187	0.188
Mn	0.003	0.0029	0.0025	0.0029
Ca	0.0006	0.0006	0.0004	0.0005
Ni	0.007	0.0075	0.0069	0.0078
Total	3.0013	2.9883	2.9928	3.0026
%Mg**	90.2	90.3	90.5	90.6

Sample*:

He3(1)(i): Olivine from an interlocking framework of extended hopper with budding olivines, with interstitial SP and OP (Rothstein, 1981).

He3 (2)M: Olivine from an aggregate immediately adjacent to He3 (2)H, which is an analysis of a discrete olivine hopper. The latter is enclosed in OP.

Hb(1): Olivine analysis from sets of spots including olivines both completely and partially enclosed in OP.

%Mg**: % Mg/(Mg + Fe)

Note: The new olivine and pyroxene analyses from He (3) and Hb, Tables 1 & 2, are from microprobe analyses by Dr.N.R. Charnley at the Department of Earth Sciences, Oxford University. These were obtained by W.D.S. using a Microscan 9, with counting errors less than 1% for major elements.

Table 1. Olivine compositions from He3 and Hb.

LOC.	H	H	H	H
Sample	He3(j)	He3(k)	Hb(m)	Hb(n)
Spots	5	10	32	15
Pyroxen	(Ca-)	(Ca+)	(Ca-)	(Ca+)
e				
SiO ₂	54.28	50.73	54.78	50.88
Al ₂ O ₃	4.3	5.13	3.58	4.58
TiO ₂	0.07	0.2	0.1	0.23
Cr ₂ O ₃	0.72	0.97	0.9	1.34
MgO	30.86	16.69	31.68	16.67
FeO	6.16	2.93	5.93	2.89
MnO	0.13	0.1	0.14	0.1
CaO	1.52	21.16	1.86	21.13
Na ₂ O	0.03	0.31	0.06	0.3
NiO	0.07	0.04	0.1	0.05
Total	98.14	98.26	99.13	98.17
Si	1.9148	1.8741	1.916	1.8831
Al	0.1789	0.2232	0.1477	0.1995
Ti	0.0017	0.0055	0.0027	0.0063
Cr	0.02	0.0283	0.0247	0.0392
Mg	1.6222	0.9194	1.6515	0.9199
Fe	0.1817	0.0905	0.1735	0.0895
Mn	0.0039	0.0032	0.004	0.003
Ca	0.0574	0.838	0.0696	0.8379
Na	0.0018	0.0218	0.004	0.0204
Ni	0.0018	0.0009	0.0028	0.0027
Total	3.9842	4.0049	3.9965	4.0015
%Mg*	89.9	91	90.5	91.1
%Ca*	3.4	47.7	4	47.7
T(M 80)		1066(k)		1061(n)
T(WS91)	1091(j)		1123(m)	
T(W77)	1062	(j&k)	1060	(m&n)

%Mg*: % Mg/(Mg + Fe)

%Ca*: %Ca/(Ca + Mg)

M80: Mercier (1980)

WS91: Witt-Eikschien and Seck (1991)

W77: Wells (1977)

Table 2. Pyroxene compositions from He3 and Hb.

textural evidence the pyroxenites appear to be part of a crystallization sequence rather than a separate injection; the relatively coarse grained pyroxenes of He2 being closely linked texturally with the preceding and succeeding Harzburgites He1 and He3 (Rothstein, 1977). The values obtained for He2, 1200° C ± 70° C are considered to be relic maxima of an initial equilibration (Rothstein, 1988).

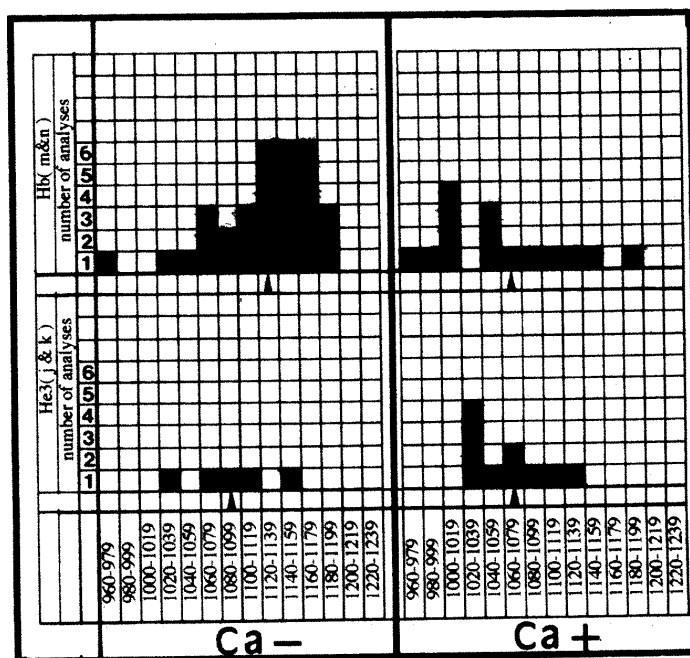


Figure 5. Spot temperatures of pyroxene equilibration

DISCUSSION

The Composition of the Olivine

As olivine is the major constituent of the primary mineral assemblage, only small changes in its Mg/Fe ratio will have occurred as the equilibration temperatures declined (Irvine, 1967). The range of the probe values for wt% Ni v. wt% Mg for He3 and Hb shown on Fig. 4 fall inside the field indicated for plutonic igneous rocks (Simkin and Smith 1970). The analysed olivines associated with the primary textures can also be compared with the olivine compositions from natural melts which have crystallised rapidly, such as the olivines of komatiites. The Lizard olivines analysed above (see Table 1), show a somewhat lower wt% NiO content of between 0.35 and 0.40 compared to the range of 0.40 to 0.55 for olivines from spinifex textured komatiites from the average analyses quoted by Donaldson (1982). Characteristically for non-komatiitic terrestrial olivines, however, the Lizard olivines have a markedly lower wt% Cr₂O₃ content of between 0.02 to 0.03 compared to the range of 0.15 to 0.33 for komatiitic olivines. This point is supported by the previously published spinel analyses for the whole range of primary assemblage peridotites (Rothstein, 1998). The spinel compositions, while both close to that of alpine type peridotites and to the range from oceanic cumulates to moderately depleted oceanic tectonites, fall outside the field of komatiitic spinels (Zhou and Kerrich, 1992) which have higher Cr₂O₃ values.

Morphology of the Olivine and Evidence for Supercooling

It has been noted previously (Rothstein, 1981) that the microcrescumulates show some resemblances to the olivine crescumulates found in ultrabasic plutonic rocks, such as those of Rhum (Brown, 1956), although the microcrescumulates are on a very much finer scale. It can also be noted that there are resemblances in some of the textures showing flared olivine crystals to the much coarser flared K-feldspar crystals found in granitic rocks, such as those of St. Michael's Mount, Cornwall (the nature and origin of which have been described and discussed in detail by Jackson and Power [1995]).

However, the closest resemblances of the microcrescumulate olivine morphologies are to those illustrated for olivine samples taken near the margin of picritic sills (Dreyer and Johnston, 1957) and those obtained experimentally by the supercooled crystallisation of mafic and ultramafic melts (Donaldson, 1976, 1977). These latter include flared olivine crystals (Donaldson, 1977, Figs 4 to 6). Equally polyhedral and hopper olivines are common in komatiites. Furthermore, the spinels from the olivine microcrescumulates at H, in showing some morphological similarities with these textural features of the olivine, indicate a process operating during the precipitation of the olivine and spinel which ceased to operate during the crystallization of the pyroxene.

The diverse morphological features of the microcrescumulates can be related to the precipitation of small euhedral olivines followed by a moderate degree of supercooling giving rise to hopper and branching olivines. A full discussion of the consequences of supercooling in melts is to be found in Donaldson (1976, 1977), Kuroda *et al* (1987) and Sunagawa (1987). The morphological changes associated with different degrees of supercooling are illustrated in the combined phase and morphology diagram in Fig. 6 (this figure is based upon Sunagawa [1987, Fig. 10]). A crystallization path associated with supercooling can explain the changes in morphology of the olivine from polyhedral to hopper within the layer He3, and also the associated morphological variations in the spinel. Thus, while polyhedral spinel is associated with the pyroxenite He2, in contrast this is followed by the sparse examples of hopper/dendritic spinel in the succeeding harzburgite He3. This latter feature could indicate a temporary incursion by the crystallizing melt of He3 into the field of

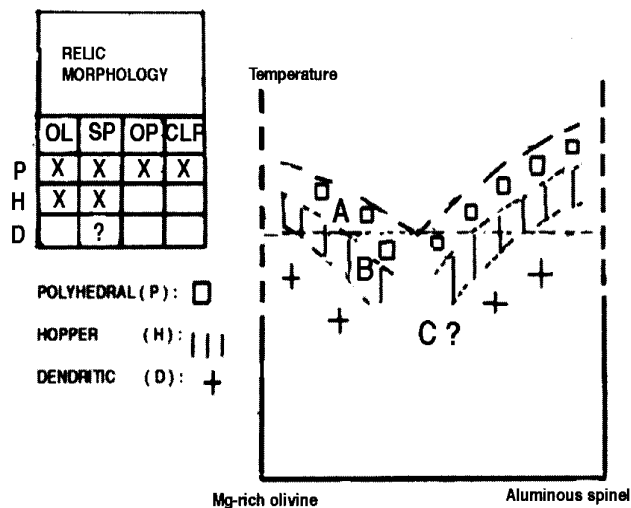


Figure 6. Morphology and supercooling illustrated on a phase diagram for olivine and spinel

supercooled spinel following a precipitation in quantity of hopper olivine.

Some of the olivine in the layer He3 has the morphology of extended crystals set at a steep angle to S_0 , and shows budding. The morphology of the olivine from a different sample of this layer includes a considerable quantity of relatively small polyhedral and hopper crystals. This equally indicates an oscillation about the boundary between polyhedral and hopper morphologies, in addition to the precipitation of a considerable quantity of olivine. The pyroxenes, being at the lower temperature, end-stage of a crystallization sequence, show relics of a polyhedral morphology and enclose the already precipitated euhedral spinel. There is also evidence of a reaction relation of the olivine to the melt, both in the resorbed character of some of the olivine crystals and in this mineral being absent from the pyroxenite assemblage. This could be expected from the system Forsterite-Diopside-Silica at high water pressure (Kushiro, 1969).

The Extent and Origin of the Primary Mineralogical Banding

Green (1964b, Fig. 1) shows on a structural map of the Lizard Peridotite the near vertical foliation or flow banding striking E. of N. roughly parallel to the coast south of Coverack (location G, Fig. 1A). Along this coast there are many outcrops of interbanded dunite and harzburgite, the best exposed of the outcrops being at Perprean Cove, Coverack. Effectively there is a 2 km section along the strike while that between H3 and Z is within a 1 km. section across the strike.

While the above is not an argument for a single unit of interbanded dunite/harzburgite layers to the south of Coverack, it suggests the existence of a zone in which such interbanding occurs. Furthermore, the direction of development between H3 and Z can be compared with the direction of development in this interbanded zone. Thus at Perprean Cove the sequence of rock types resembles that at Z (see Rothstein, 1977, Fig. 1; 1981, Fig. 1), but some of the evidence in the disposition of some of the spinel trails indicates that the direction of development of the layers at this locality may be reversed compared to that found at localities H3, H, and Z. There is not, however, enough detailed information available on the variation in the microtextures along, and across the strike on the coast to the south of Coverack to be able to make observations comparable to those that have been made between H3 and Z. The evidence, so far, is that there are many highly deformed rocks in this zone (Rothstein, 1981, Fig. 1).

While supercooling could be characteristic of the section H3 to Z, other primary textures could have been present along the strike of the banded zone south of Coverack. It is necessary to determine the nature of any such microtextures and associated olivine compositions before the full character of the mineralogical banding in this part of the primary assemblage peridotite can be fully assessed.

Nevertheless, even allowing for the above limitations, it is possible to suggest a working hypothesis for the origin of the primary olivine and spinel precipitate. This is that the precipitate includes both cumulate and microcrescumulate layers, these latter including a sequence of polyhedral and hopper crystals with a complex range of morphologies and textures, as well as the development of aggregates in which the continued crystallization of olivine formed abutting crystals with a granular texture. Furthermore, the banded sequence of microcrescumulate layers was produced by the sequential supercooling of high temperature/high pressure liquids crystallizing as thin sheets (the latter consideration permitting a relatively rapid loss of heat). This precipitate was porous and within it a pyroxene rich residual liquid was able to percolate, partially resorb some of the olivine, and eventually crystallize in extreme cases as pyroxenite. Following the initial re-equilibration of the textures the completely crystallized banded rock was folded (possibly), deformed, and recrystallized under conditions of declining pressure and temperature.

CONCLUSIONS

I have argued previously that there is evidence that the primary assemblage peridotite contains textural relics of an early igneous event. It is concluded from this new work that the precipitation of the olivine has occurred under conditions of moderate supercooling *in situ*, based on the evidence from those parts of the banded sequences in which primary textures are well preserved, and in which microcrescumulates are present. This process produced unusual complex primary textures constructed from both polyhedral and hopper olivines. This event occurred at pressures and temperatures characteristic of the spinel-lherzolite facies of the sub-oceanic upper mantle. In the samples analysed, the olivine appears to be consistent with precipitation from a non-komatiitic suite of ultramafic melts.

REFERENCES

- BROWN, G.M. 1956. The Layered Ultrabasic Rocks of Rhum, Inner Hebrides. *Philosophical Transactions of the Royal Society. Series B*, **240**, 1-53.
- COOK, CA, HOLDSWORTH, R. E. and STYLES, M.T. 1998. The tectonic evolution of peridotites in the Lizard Ophiolite Complex, South-West England. *Geoscience in South-West England*, **9**, 182-187.
- DAVIES, G.R. 1984. Isotopic evolution of the Lizard Complex *Journal of the Geological Society of London*, **141**, 3-14.
- DONALDSON, C.H. 1976. An experimental investigation of olivine morphology. *Contributions to Mineralogy and Petrology*, **57**, 187-213.
- DONALDSON, C.H. 1977. Laboratory duplication of comb layering in the Rhum pluton. *Mineralogical Magazine*, **41**, 323-336.
- DONALDSON, C.H. 1982. Spinifex-textured komatiites: a review of textures, compositions and layering. In: *Komatiites*. Eds: N.T. Arntd and E. Nisbet, London, G.Allen & Unwin, PP 213-214
- DREVER, H.I. and JOHNSTONE, R.1957. Crystal growth of forsteritic olivine in magmas and melts. *Transactions of the Royal Society of Edinburgh*, **LXIII**, pt II, 289-315
- FLEET, J.S. 1946. The geology of the Lizard and Menage. *Memoir of the Geological Survey*. Sheet 359. 2nd edition, London: HMSO.
- GREEN, D.H. 1964a. The petrogenesis of the high-temperature peridotite in the Lizard area, Cornwall. *Journal of Petrology*, **5**, (1), 134-188.
- GREEN, D.H. 1964b. The metamorphic aureole of the peridotite at the Lizard, Cornwall. *Journal of Geology*, **72**, 543-563.
- IRVINE, T.N. 1967. Chromian spinel as a petrogenetic indicator. part 2: petrologic applications. *Canadian Journal of Earth Sciences*, **4**, 71-103.
- JACKSON, G.EA. and POWER, G.M. 1995. Columnar, branching, and curved feldspar growth in the St. Michael's Mount Granite, Cornwall. *Proceedings of the Ussher Society*, **8**, 363-367.
- KURODA, T, IRISAWA,T and OOKAWA, A.1987. Transition from polyhedral to dendritic morphology. In: *Morphology of Crystals*. Ed. I. Sunagawa, Tokyo, Terra Scientific Publishing Company, PP 591-612.
- KUSHIRO, I. 1969. The system Forsterite-diopside-Silica with and without water at high pressures. *American Journal of Science. Schairer*, **267-A**, 269-294.
- MERCIER, J-C.C. 1980. Single-pyroxene thermobarometry. *Tectonophysics*, **70**, 1-37.
- ROTHSTEIN, A.T.V. 1977. The distribution and origin of primary textures in the Lizard Peridotite, Cornwall. *Proceedings of the Geologists' Association*, **88**, (2), 93-105.
- ROTHSTEIN, A.T.V. 1981. The primary crescumulates of the Lizard Peridotite, Cornwall. *Geological Magazine*, **118**, (5), 491-500.
- ROTHSTEIN, A.T.V. 1988. An analysis of the textures within the primary assemblage peridotite, the Lizard, Cornwall. *Proceedings of the Geologists' Association*, **99**, (3), 181-192.
- ROTHSTEIN, A.T.V. 1994. Directional features within an assemblage of primary textures preserved in a kilometre section of the upper mantle peridotite, from the Lizard, Cornwall. *Proceedings of the Ussher Society*, **8**, 248-253.
- ROTHSTEIN, A.T.V. 1998. Relic primary features of the spinel-bearing dunites of the primary assemblage peridotite, the Lizard, Cornwall. *Geoscience in South-West England*, **9**, 178-181.
- SIMKIN, T. and SMITH, J.V. 1970. Minor-element distribution in olivine. *Journal of Geology*, **78**, 304-325.
- SUNAGAWA, I. 1987. Morphology of minerals. In: *Morphology of Crystals*. Ed. I. Sunagawa, Tokyo, Terra Scientific Publishing Company, PP 511-587.
- WELLS, P.R.A. 1977. Pyroxene thermometry in simple and complex systems. *Contributions to Mineralogy and Petrology*, **62**, 129-139.
- WITT-EIKSCHEN, G. and SECK, H.A. 1991. Solubility of Ca and Al in orthopyroxene from spinel-peridotite: an improved version of an empirical geothermometer. *Contributions to Mineralogy and Petrology*, **106**, 431-439.
- ZHOU, M. and KERRICH, R 1992. Morphology and composition of chromite in Komatiites from the Belingwe Geenstone belt, Zimbabwe. *Canadian Mineralogist*, **30**, 303-317.

EDITOR'S NOTE

Some of the figures in this contribution were not perfect but the decision was taken to publish this paper as a tribute to the author who sadly passed away this year.